Eur. Phys. J. B **62**, 71–76 (2008)
DOI: 10.1140/epjb/e2008-00130-1

THE EUROPEAN PHYSICAL JOURNAL B

Spin pump effects on the spin current through two coupled quantum dots

H. Pan[1,2,a], S.-Q. Duan[2,b], L.-N. Zhao[3], W.-D. Chu[2], and W. Zhang[2]

[1] Department of Physics, Beijing University of Aeronautics and Astronautics, Beijing 100083, P.R. China
[2] Institute of Applied Physics and Computational Mathematics, Beijing 100088, P.R. China
[3] Atomistix Asia Pacific Pte Ltd, Unit 106, Innovation Center Block 1, 16 NanYang Drive, 637722, Singapore

Received 6 January 2008 / Received in final form 2 March 2008
Published online 28 March 2008 –

Abstract. We theoretically study the spin pump effects of the rotating magnetic field on the spin current through two coupled quantum dots. Owing to the interdot coupling, two molecular states with different bands can be formed, resulting asymmetric spin current peaks. The possibility of manipulating the spin current is explored by tuning the strength, the frequency, and the direction of the rotating magnetic field. The number and location of the spin current peaks can be controlled by making use of various tunings. Furthermore, the normal 2π period of the spin current with respect to the magnetic flux can be destroyed by the interdot coupling.

PACS. 73.63.-b Electronic transport in nanoscale materials and structures – 72.25.Mk Spin transport through interfaces – 85.75.-d Magnetoelectronics; spintronics: devices exploiting spin polarized transport or integrated magnetic fields – 85.65.+h Molecular electronic devices

1 Introduction

Recently, many research efforts have been devoted to generating the pure spin current without an accompanying charge current, since one of the key ingredients in spintronics is to use and control the spin current in the nonlinear electronic devices [1]. Therefore, it becomes a very important problem in spintronics to understand and exploit various physical mechanisms to generate spin current in solid state devices. Experimentally, the realization of the spin current has been reported by tuning the confining potential of the quantum dot and the external magnetic field [2]. The optical-controlled injection of pure spin current has also been realized experimentally in semiconductors [3–5]. Theoretically, a number of proposals to generate a pure spin current have been proposed by using the confining potential of quantum dots [6], the pumping frequency [7], the magnetic barriers [8], the rotating magnetic fields [9,10], and the Rashba spin-orbit coupling [11].

On the other hand, the series- and parallel-coupled double quantum dot (DQD) system has attracted much attention recently, since it makes the quantum transport phenomena rich and varied. The parallel-coupled DQD system is of particular interest, in which two coupled QDs are embedded into opposite arms of the AB ring [12,13]. As a controllable two-level system, the DQD system therefore becomes one of the promising candidates as a quantum bit in quantum computation based on solid-state devices [14]. Inspired by these recent experiments, several groups have attempted to address this parallel-coupled DQD system theoretically and predicted the existence of the Fano resonance [15,16]. Due to the interdot coupling, the two QD states can form two molecule states. The influence of the interdot coupling on the pure spin current is still not clear. It is certainly of practical importance to control the spin current in the parallel-coupled DQD system. Although the AB interference of the charge current has been well studied in a DQD system, its influence on the spin current is equally significant, since the rotating magnetic field provides a spin-flip mechanism during the resonant tunneling.

In this paper, we investigate the spin pump effects on the parallel-coupled DQD system connected by two normal-metal (N) leads. In this N-DQD-N system, two quantum dots coupled to each other via barrier tunneling are embedded into opposite arms of an AB ring, respectively. The spin pump is facilitated by a rotating magnetic field which induces the spin-flip effects. Then the spin current is generated, since the spin pump can be employed as a spin generator [10]. The magnetic field rotates around $\hat{z}$ axis with a tilt angle θ as: $\mathbf{B}(t) = (B_0 \sin\theta\cos\omega t, B_0 \sin\theta \sin\omega t, B_0\cos\theta + B_1)$, where B_0 and B_1 are the constant magnetic field strengths. The rotating components $(B_0 \sin\theta\cos\omega t,\ B_0 \sin\theta \sin\omega t)$ in the $\hat{x}$-$\hat{y}$ plane provide a spin flip mechanism. The $\hat{z}$ component $B_z = B_0\cos\theta + B_1$ gives the Zeeman split and the magnetic flux through the AB ring.

[a] e-mail: hpan@buaa.edu.cn
[b] e-mail: duan_suqing@iapcm.ac.cn

With the help of nonequilibrium Green's function (NGF) techniques [17–19], we have analyzed the tunable spin current through this DQD system. Our results show that two molecular states of the system can be formed due to the interdot coupling. Since the two states have different band widths, the spin current shows an asymmetric structure, which is quite different from the single N-QD-N system. The number and location of the spin current peaks can be controlled by making use of various tunings, such as the strength, the frequency, and the direction of the rotating magnetic field. Furthermore, the normal 2π period of the spin current with respect to the magnetic flux can be destroyed by the interdot coupling. The rest of this paper is organized as follows. In In Section 2 we present the model Hamiltonian and derive the formula of the spin current by using the NGF technique. In Section 3 we study the spin current by tuning various parameters. The interdot coupling effects on the spin current are discussed in detail. Finally, a brief summary is given in Section 4.

2 Physical model and formula

The N-DQD-N system with a rotating magnetic field is described by the following Hamiltonian:

$$H = \sum_{\alpha=L,R} H_\alpha + H_{dot} + H'(t) + H_T, \tag{1}$$

with

$$H_\alpha = \sum_{k\sigma} \epsilon_{\alpha,k} a^\dagger_{\alpha,k\sigma} a_{\alpha,k\sigma}, \tag{2}$$

$$H_{dot} = \sum_{\sigma,i=1,2} (\varepsilon_i - eV_{gi} + \sigma\mu_B B_z) d^\dagger_{i\sigma} d_{i\sigma} - \sum_{\sigma} (t_c e^{i\varphi} d^\dagger_{1\sigma} d_{2\sigma} + H.c.), \tag{3}$$

$$H'(t) = \sum_{i=1,2} \gamma e^{-i\omega t} d^\dagger_{i\uparrow} d_{i\downarrow} + H.c., \tag{4}$$

$$H_T = \sum_{\alpha,k\sigma,i=1,2} t_{\alpha i} d^\dagger_{i\sigma} a_{\alpha,k\sigma} + H.c. \tag{5}$$

H_α ($\alpha = L, R$) describes the left and right normal metal leads. H_{dot} models the parallel-coupled double quantum dots where $d^\dagger_{i\sigma}$ ($d_{i\sigma}$) represents the creation (annihilation) operator of the electron with energy ε_i in the dot i ($i = 1, 2$). The DQD energy levels can be changed by the gate voltage V_{gi}. μ_B is the Bohr magneton. t_c denotes the interdot coupling strength, and φ denotes a phase shift related to the flux difference between the left and right subrings. H' is the off diagonal part of the Hamiltonian due to the rotating magnetic field with the Rabi frequency $\gamma = \mu_B B_0 \sin\theta$. H_T represents the tunneling coupling between the DQD and leads, and the tunneling matrix elements are set as $t_{L1} = |t_{L1}|e^{i\phi/4}$, $t_{L2} = |t_{L2}|e^{-i\phi/4}$, $t_{R1} = |t_{R1}|e^{-i\phi/4}$, and $t_{R2} = |t_{R2}|e^{i\phi/4}$. The phase shift due to the magnetic flux threading into the AB ring is assumed to be $\phi = 2\pi B_z S/\phi_0 = 2\pi(\phi_R + \phi_L)/\phi_0$ with the flux quantum $\phi_0 = hc/e$ and the area S of the AB ring. $\phi_{L/R}$ is the magnetic flux threading the left/right subring. The difference between the two parts of magnetic fluxes is $\varphi = \pi(\phi_R - \phi_L)/\phi_0$. In the model above, only the coupling between the magnetic field and the spin degrees of freedom are considered. Since time-dependent magnetic field rotates in the in the $\hat{x}$-$\hat{y}$ plane, its $\hat{z}$ component is a time independent constant. Therefore, the magnetic flux due to the time-dependent rotating components of the magnetic field is zero [10].

The charge and spin current can be calculated analytically by using the NGF method. The spin current is defined as $I^s = -\frac{\hbar}{2}(I_\uparrow - I_\downarrow)$ and the charge current is defined as $I^e = e(I_\uparrow + I_\downarrow)$ where I_σ is the electron current with spin $\sigma = \pm 1 = \uparrow, \downarrow$ [10]. The charge current I^e_α and spin current I^s_α from the α lead to the central region can be calculated from standard NGF techniques and can be expressed in terms of the dot's Green's function as [17]

$$I^{e,s}_\alpha(t) = \frac{2}{\hbar}\mathrm{Re}\int dt' \mathrm{Tr}\{\sigma_{e,s}[\mathbf{G}^<(t,t')\mathbf{\Sigma}^a_\alpha(t',t) + \mathbf{G}^r(t,t')\mathbf{\Sigma}^<_\alpha(t',t)]\}, \tag{6}$$

where σ_e and σ_s are defined as follows

$$\sigma_e = e\begin{pmatrix} 1&0&0&0\\ 0&1&0&0\\ 0&0&1&0\\ 0&0&0&1 \end{pmatrix}, \quad \sigma_s = -\frac{\hbar}{2}\begin{pmatrix} 1&0&0&0\\ 0&-1&0&0\\ 0&0&1&0\\ 0&0&0&-1 \end{pmatrix}. \tag{7}$$

The retarded Green's functions are defined as $\mathbf{G}^r(t,t') = -i\theta(t-t')\langle\{\Psi(t), \Psi^\dagger(t')\}\rangle$ and $\mathbf{G}^<(t,t') = i\langle\Psi^\dagger(t')\Psi(t)\rangle$, respectively, with the operator $\Psi = (d^\dagger_{1\uparrow}, d^\dagger_{1\downarrow}, d^\dagger_{2\uparrow}, d^\dagger_{2\downarrow})^\dagger$. In general, to solve a time-dependent problem needs some perturbation theory. Fortunately, $\mathbf{G}^r(t,t')$ can be solved exactly for the time-dependent Hamiltonian considered here [10]. First, it is simple to calculate the retarded Green's function for the diagonal part (in spin space) of the Hamiltonian. Then, the retarded Green's functions under the rotating magnetic field $H'(t)$ can be calculated by using Dyson equation

$$\mathbf{G}^r(t,t') = \mathbf{G}^{0r}(t-t') + \int dt_1 \mathbf{G}^r(t,t_1) \times \mathbf{H}'(t_1)\mathbf{G}^{0r}(t_1 - t'), \tag{8}$$

where $\mathbf{G}^{0r}$ is the retarded Green's function without the rotating magnetic field and $\mathbf{H}'$ is given by

$$\mathbf{H}'(t) = \begin{pmatrix} 0 & \gamma e^{-i\omega t} & 0 & 0\\ \gamma e^{i\omega t} & 0 & 0 & 0\\ 0 & 0 & 0 & \gamma e^{-i\omega t}\\ 0 & 0 & \gamma e^{i\omega t} & 0 \end{pmatrix}. \tag{9}$$

The lesser Green's functions can be calculated by using Keldysh equation

$$\mathbf{G}^{<}(t,t') = \int dt_1 dt_2 \mathbf{G}^{r}(t,t_1)\mathbf{\Sigma}^{<}(t_1-t_2)\mathbf{G}^{a}(t_2,t'). \quad (10)$$

After the double Fourier transform over time t and t',

$$\mathbf{G}(\epsilon,\epsilon') = \int dt dt' e^{i\epsilon t - i\epsilon t'}\mathbf{G}(t,t'). \quad (11)$$

The equations for the Green's function are

$$\begin{aligned}
\mathbf{G}^{r}_{11}(\epsilon,\epsilon') &= 2\pi\mathbf{G}^{0r}_{11}(\epsilon)\delta(\epsilon-\epsilon') + \gamma\mathbf{G}^{r}_{12}(\epsilon,\epsilon'-\omega)\mathbf{G}^{0r}_{11}(\epsilon') \\
&\quad + \gamma\mathbf{G}^{r}_{14}(\epsilon,\epsilon'-\omega)\mathbf{G}^{0r}_{31}(\epsilon'), \quad (12)\\
\mathbf{G}^{r}_{12}(\epsilon,\epsilon') &= \gamma\mathbf{G}^{r}_{11}(\epsilon,\epsilon'+\omega)\mathbf{G}^{0r}_{22}(\epsilon') \\
&\quad + \gamma\mathbf{G}^{r}_{13}(\epsilon,\epsilon'+\omega)\mathbf{G}^{0r}_{42}(\epsilon'), \quad (13)\\
\mathbf{G}^{r}_{13}(\epsilon,\epsilon') &= 2\pi\mathbf{G}^{0r}_{13}(\epsilon)\delta(\epsilon-\epsilon') \\
&\quad + \gamma\mathbf{G}^{r}_{12}(\epsilon,\epsilon'-\omega)\mathbf{G}^{0r}_{13}(\epsilon') \\
&\quad + \gamma\mathbf{G}^{r}_{14}(\epsilon,\epsilon'-\omega)\mathbf{G}^{0r}_{33}(\epsilon'), \quad (14)\\
\mathbf{G}^{r}_{14}(\epsilon,\epsilon') &= \gamma\mathbf{G}^{r}_{11}(\epsilon,\epsilon'+\omega)\mathbf{G}^{0r}_{24}(\epsilon') \\
&\quad + \gamma\mathbf{G}^{r}_{13}(\epsilon,\epsilon'+\omega)\mathbf{G}^{0r}_{44}(\epsilon'). \quad (15)
\end{aligned}$$

Shifting the variable ϵ' to $\epsilon'-\omega$ in equations (13) and (15) and then substituting into equations (12) and (14), we can solve for $\mathbf{G}^{r}_{ij}(\epsilon,\epsilon')$ with $i=1$ and $j=1,2,3,4$. The other matrix elements of $\mathbf{G}^{r}$ can be calculated in a similar way. It is noted that the rotating magnetic field facilitates the solution in terms of the matrix Green's functions. Otherwise, it would lead to a set of equations that do not close. The Green's functions without the rotating magnetic fields $\mathbf{G}^{0r}(\epsilon)$ can be obtained as

$$\mathbf{G}^{0r}(\epsilon) = [\mathbf{g}^{r}(\epsilon)^{-1} - \mathbf{\Sigma}^{r}(\epsilon)]^{-1}, \quad (16)$$

where $\mathbf{g}^{r}(\epsilon)$ is the Green's function of the QD without the coupling to the leads

$$[\mathbf{g}^{r}(\epsilon)]^{-1} = \begin{pmatrix} \epsilon-\varepsilon_{1\uparrow}+i0^{+} & 0 & t_c e^{i\varphi} & 0 \\ 0 & \epsilon-\varepsilon_{1\downarrow}+i0^{+} & 0 & t_c e^{i\varphi} \\ t_c e^{-i\varphi} & 0 & \epsilon-\varepsilon_{2\uparrow}+i0^{+} & 0 \\ 0 & t_c e^{-i\varphi} & 0 & \epsilon-\varepsilon_{2\downarrow}+i0^{+} \end{pmatrix}, \quad (17)$$

where the energy level ε_i is split into $\varepsilon_{i\downarrow} = \varepsilon_i - \mu_B B_z$ and $\varepsilon_{i\uparrow} = \varepsilon_i + \mu_B B_z$ due to Zeeman splitting. The self energy is $\mathbf{\Sigma}^{r}(\epsilon) = \mathbf{\Sigma}^{r}_{L}(\epsilon) + \mathbf{\Sigma}^{r}_{R}(\epsilon)$. Under the wide-bandwidth approximation, the retarded self-energy can be derived as

$$\mathbf{\Sigma}^{r}_{\alpha}(\epsilon) = -\frac{i}{2}\begin{pmatrix} \Gamma^{\alpha}_{1} & 0 & \sqrt{\Gamma^{\alpha}_{1}\Gamma^{\alpha}_{2}}e^{i\Phi_\alpha} & 0 \\ 0 & \Gamma^{\alpha}_{1} & 0 & \sqrt{\Gamma^{\alpha}_{1}\Gamma^{\alpha}_{2}}e^{i\Phi_\alpha} \\ \sqrt{\Gamma^{\alpha}_{1}\Gamma^{\alpha}_{2}}e^{-i\Phi_\alpha} & 0 & \Gamma^{\alpha}_{2} & 0 \\ 0 & \sqrt{\Gamma^{\alpha}_{1}\Gamma^{\alpha}_{2}}e^{-i\Phi_\alpha} & 0 & \Gamma^{\alpha}_{2} \end{pmatrix}, \quad (18)$$

where $\Phi_\alpha = \pm\phi/2$ ($\alpha = L/R$). The linewidth function is defined as $\Gamma^{\alpha}_{i} = 2\pi\rho_\alpha t^{*}_{\alpha i}t_{\alpha i}$ with ρ_α being the density of states of the corresponding α lead, describing the coupling between the ith QD and the α lead. Once the retarded Green's functions are obtained, the lesser Green's function can be obtained as

$$\mathbf{G}^{<}(\epsilon,\epsilon') = \int \frac{d\epsilon_1}{2\pi}\mathbf{G}^{r}(\epsilon,\epsilon_1)\mathbf{\Sigma}^{<}(\epsilon_1)\mathbf{G}^{a}(\epsilon_1,\epsilon'), \quad (19)$$

where $\mathbf{\Sigma}^{<}(\epsilon) = \mathbf{\Sigma}^{<}_{L}(\epsilon) + \mathbf{\Sigma}^{<}_{R}(\epsilon)$ with $\mathbf{\Sigma}^{<}_{L,R} = f_{L,R}(\mathbf{\Sigma}^{a}_{L,R} - \mathbf{\Sigma}^{r}_{L,R})$ and $f_{L,R}(\epsilon) = 1/(e^{(\epsilon-\mu_{L,R})/k_BT}+1)$ the Fermi distribution function of the leads. With these Green's functions, the Fourier transform of the averaged current in one period is given by

$$I^{e,s}_{\alpha} = -\frac{2}{\hbar}\mathrm{Re}\int\frac{d\epsilon}{2\pi}\mathrm{Tr}\{\hat{\sigma}_{e,s}[\mathbf{G}^{<}(\epsilon,\epsilon)\mathbf{\Sigma}^{a}_{\alpha}(\epsilon) + \mathbf{G}^{r}(\epsilon,\epsilon)\mathbf{\Sigma}^{<}_{\alpha}(\epsilon)]\}. \quad (20)$$

In the following, we perform the calculations at zero temperature in units of $\hbar = e = 1$ and focus on the spin current at zero bias. The couplings between the quantum dots and leads are set as $\Gamma^{\alpha}_{1} = \Gamma^{\alpha}_{2} = \Gamma_\alpha = \Gamma/2 = 0.1$. The energy and the spin current are scaled by Γ, whose typical values in experiments are of the order of tens of μeV [20].

3 Numerical results and discussions

To make the physical picture clear, the two coupled QD levels can be transformed into two decoupled states of the DQD molecule. When the magnetic field is zero, the operator for a molecular state can be expressed as a linear superposition of the QD operators as

$$\begin{pmatrix} \tilde{d}_{+} \\ \tilde{d}_{-} \end{pmatrix} = \begin{pmatrix} \cos\beta e^{-i\varphi} & -\sin\beta \\ \sin\beta & \cos\beta e^{i\varphi} \end{pmatrix}\begin{pmatrix} d_1 \\ d_2 \end{pmatrix}, \quad (21)$$

where $\tilde{d}_{-}$ and $\tilde{d}_{+}$ are referred to as the annihilation operators for the bonding and antibonding states of the QD molecule, and $\beta = 1/2\tan^{-1}[2t_c/(\varepsilon_1-\varepsilon_2)]$. Thus, the Hamiltonian for the coupled double quantum dot H_D is diagonalized as $\tilde{H}_D = \varepsilon_{+}\tilde{d}^{\dagger}_{+}\tilde{d}_{+} + \varepsilon_{-}\tilde{d}^{\dagger}_{-}\tilde{d}_{-}$, where $\varepsilon_{\pm} = \frac{1}{2}[\varepsilon_1+\varepsilon_2 \pm \sqrt{(\varepsilon_1-\varepsilon_2)^2+4t_c^2}]$. The linewidth matrix corresponding to the two states coupled to the left lead are respectively

$$\begin{aligned}
\Gamma^{L}_{+} &= \Gamma^{L}_{1}\cos^2\beta + \Gamma^{L}_{2}\sin^2\beta \\
&\quad - \sqrt{\Gamma^{L}_{1}\Gamma^{L}_{2}}\sin(2\beta)\cos\left(\frac{\phi}{2}-\varphi\right), \quad (22)
\end{aligned}$$

and

$$\begin{aligned}
\Gamma^{L}_{-} &= \Gamma^{L}_{1}\sin^2\beta + \Gamma^{L}_{2}\cos^2\beta \\
&\quad + \sqrt{\Gamma^{L}_{1}\Gamma^{L}_{2}}\sin(2\beta)\cos\left(\frac{\phi}{2}-\varphi\right). \quad (23)
\end{aligned}$$

The formula for $\Gamma^{R}_{\pm}$ are the same as above except that the sign before φ is $+$. Therefore, the DQD system is mapped

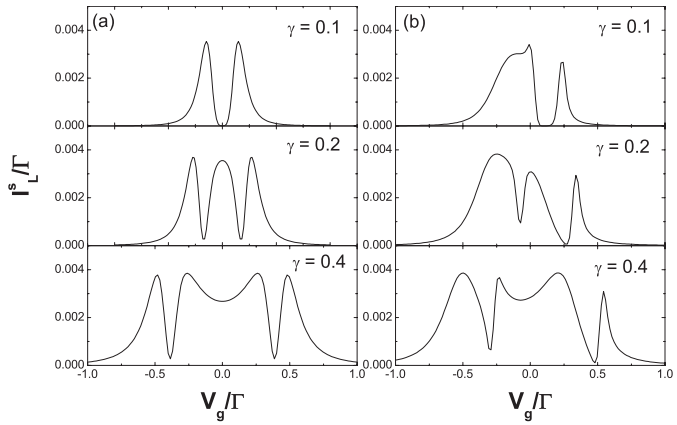

Fig. 1. I_L^s versus V_g for (a) $t_c = 0$ and (b) $t_c = 0.1$ at different γ. Other parameters are $\theta = \pi/2$, $\omega = 0.05$, $B_1 = 0$, $\varepsilon_1 = 0.1$, and $\varepsilon_2 = -0.1$.

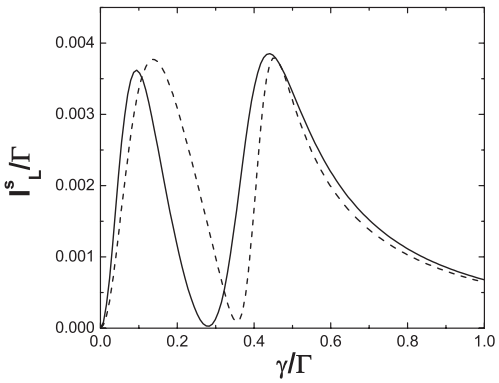

Fig. 2. I_L^s versus γ for $t_c = 0$ (solid line), and $t_c = 0.1$ (dashed line). Other parameters are $\theta = \pi/2$, $\omega = 0.05$, $B_1 = 0$, $\varepsilon_1 = 0$, and $\varepsilon_2 = 0.4$.

onto a system of two independent molecular states with band $\Gamma_{\pm}^{\alpha}$ connected to leads. The level associated with a wider band can be referred to as the strongly coupled one, while that with narrow band is referred to as the weakly coupled level. At zero bias voltage ($\mu_L = \mu_R = 0$), a spin current can be generated by the rotating magnetic field without a charge current. When a spin-down electron tunnels into one of the molecular states $\varepsilon_{\pm\downarrow}$ from the left lead, it can absorb a photon and transits to the level $\varepsilon_{\pm\uparrow}$ with its spin flipped due to the spin pump effects. This spin-up electron then tunnels out of the DQD with certain probabilities to the left and right leads. The same happens to spin-down electrons in the right lead exactly. The average outcome is that a number of spin-down electrons flow toward the QD molecule and an equal number of spin-up electrons flowing away from it. Therefore, a pure spin current is established without charge current [10]. If the rotation direction and $\hat{z}$ component of $\mathbf{B}(t)$ are reversed, the flow of spin current will also reverse.

Figure 1 shows the spin current I_L^s versus the gate voltage V_g for various γ with and without the interdot coupling t_c. When there is no coupling strength with $t_c = 0$ as shown in Figure 1a, the pure spin current under different field strength γ exhibits a symmetric structure. Under the weak external field with $\gamma = 0.1 \leq \Gamma/2$, two resonance peaks located at the two QD states with $\varepsilon_1 = 0.1$ and $\varepsilon_2 = -0.1$ are represented. With increasing the field strength γ, there appear three and four current peaks at $\gamma = 0.2$ and $\gamma = 0.4$, respectively. In the above numerical calculations, the frequency of the external fields is set as small value so that the adiabatic approximation holds. Thus the change of the current peaks can be understood from the expression of the spin current in the adiabatic regime [10]

$$I_L^s = \frac{\omega\gamma^2\Gamma^2}{4\pi[(\varepsilon^2 + \Gamma^2/4 - \gamma^2)^2 + \Gamma^2\gamma^2]}. \tag{24}$$

When $\gamma = 0.1 \leq \Gamma/2$, the spin current for each QD state has only one peak whose location depends on the level ε_i. Thus the total spin current for the two QD states shows two current peaks at ε_1 and ε_2. When $\gamma = 0.2 > \Gamma/2$, the spin current for each QD state exhibits two peaks. However, since the higher peak corresponding to $\varepsilon_2 = -0.1$ is adjacent to the lower one corresponding to $\varepsilon_1 = 0.1$, the two peaks are very close and overlapped to merge into one wider central peak, resulting in three peaks in the total spin current. When $\gamma = 0.4$, the locations of the middle two current peak are large enough to split into two. Thus the total spin current shows four peaks. When there exists the coupling strength with $t_c = 0.1$ as shown in Figure 1b, it is clearly shown that the coupling interaction results in the shift of resonance peaks. The two molecular states are formed at $\varepsilon_- = -0.14$ and $\varepsilon_+ = 0.14$ with a wide band Γ_-^L and narrow band Γ_+^L, respectively. The lower molecular state becomes wider while the higher molecular state become narrower, which can be seen from the formula for Γ_- and Γ_+. The broadening of the lower state is always accompanied by shrinking the higher state since $\Gamma_-^L + \Gamma_+^L = \Gamma_1^L + \Gamma_2^L$. The two molecular states has different lindwidth and becomes one strongly and one weakly coupled states due to the interdot coupling. Therefore, the spin current peaks exhibit an asymmetric structure under the influence of the interdot coupling.

The magnetic field strength has a distinct influence on the spin current. To clearly show this, the spin current of the left lead versus γ at $\varepsilon_1 = 0.1$ and $\varepsilon_2 = 0.5$ is plotted in Figure 2 At zero interdot coupling of $t_c = 0$, there appears two peaks in the spin current curves with increasing γ, which is quite different from that for the single QD system. The two current peaks locate at $\gamma = 0.1$ and $\gamma = 0.5$, respectively. The reason is related to the Rabi resonance caused by the rotating magnetic field with a Rabi frequency γ. Due to the rotating magnetic field, the original spin-degenerate QD state ε_i is splitted into $\tilde{\varepsilon}_{i\sigma} = \varepsilon_i \pm \gamma$. [21] When $\gamma = 0.1$, one of the two states $\tilde{\varepsilon}_{1\sigma}$ is located at the Fermi energy, resulting in one current peak. Similarly, when $\gamma = 0.5$, one of the two states $\tilde{\varepsilon}_{2\sigma}$ is located at the Fermi energy, which also leads to one current peak. At the finite interdot coupling of $t_c = 0.1$, the two peaks shift outwards, since the positions of the two molecular states $\varepsilon_{\pm}$ are different from the two QD states $\varepsilon_{1,2}$ due to the nonzero interdot coupling. Under

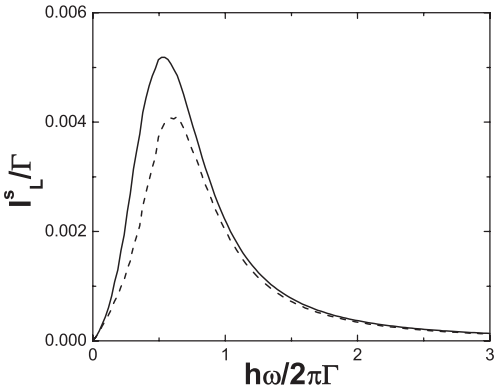

Fig. 3. I_L^s versus ω for $t_c = 0$ (solid line), and $t_c = 0.2$ (dashed line). Other parameters are $\theta = \pi/2$, $\gamma = 0.05$, $\mu_B B_1 = 0.25$, and $\varepsilon_1 = \varepsilon_2 = 0$.

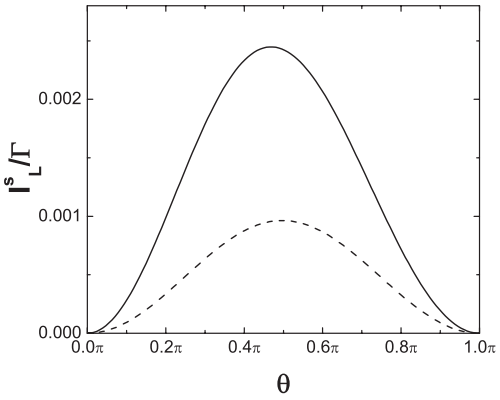

Fig. 4. I_L^s versus θ for $t_c = 0$ (solid line), and $t_c = 0.2$ (dashed line). Other parameters are $\omega = 0.05$, $\gamma = 0.1$, $B_1 = 0$, and $\varepsilon_1 = \varepsilon_2 = 0$.

the rotating magnetic field, the two molecular states also become spin dependent as $\tilde{\varepsilon}_{\pm\sigma} = \varepsilon_{\pm} \pm \gamma$. therefore, the spin current also shows the two peaks.

In order to see the Zeeman splitting effects, the spin currents versus the the field frequency ω for $\varepsilon_1 = \varepsilon_2 = 0$ with different t_c are clearly shown in Figure 3 When there is no interdot coupling at $t_c = 0$, the spin current shows a maximum value at about $\omega = 2\mu_B B_z = 0.5$ with increasing ω. Due to the Zeeman splitting caused by B_z, the energy levels of the quantum dots are not spin degenerate and become $\varepsilon_{i\uparrow} = \mu_B B_z$ and $\varepsilon_{i\downarrow} = -\mu_B B_z$, respectively. The two spin levels are coupled by the rotating magnetic field $(\gamma\cos\omega t,\ \gamma\sin\omega t)$. When $\omega = 2\mu_B B_z$, the rotating field induces the resonance between the spin-down and spin-up levels, resulting a maximum spin current. When there is a finite interdot coupling at $t_c = 0.1$, the spin current is decreased and the peak shifts outwards, since the two molecular states $\varepsilon_{\pm}$ move away from the Fermi energy.

Figure 4 depicts the spin current as a function of θ for $\varepsilon_1 = \varepsilon_2 = 0$ with different t_c. The spin current has a maximum value at $\theta = \pi/2$, since the segment of external field causing the spin pump effects reach its maximum value. With increasing t_c, the spin current decreases, because ε_+ and ε_- are shifted much further from the Fermi energy. It is also interesting to see the effect of the magnetic flux on the spin current. We now discuss the AB oscillations of the spin current as a function of magnetic flux. Figure 5 presents the dependence of the I_L^s on the magnetic flux ϕ without and with the interdot coupling. In the parallel system, there are two subring when there exists the interdot coupling t_c. This leads to complex AB oscillations for the spin current. For simplicity, we set $n = \phi_R/\phi_L = 1$. For the case of $t_c = 0$, the oscillation period of the spin current versus magnetic flux is 2π. For the cases of $t_c = 0.1$, the periods are 4π. The 4π periods agree with the period formula $2(n+1)\pi$ with $n = 1$ [22]. It means that the normal AB oscillations with a period of 2π can be destroyed and complex periodic oscillations are generated.

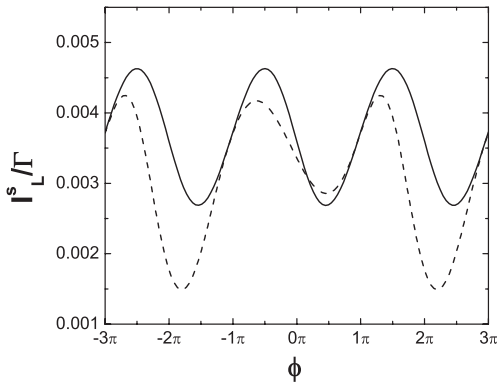

Fig. 5. I_L^s versus ϕ for $t_c = 0$ (solid line) and $t_c = 0.1$ (dashed line). Other parameters are $\theta = \pi/2$, $\omega = 0.05$, $\gamma = 0.1$, $\varepsilon_1 = 0$, and $\varepsilon_2 = 0.4$.

4 Summary

In summary, we have theoretically studied the spin pump effects caused by the rotating magnetic field on the electron transport through a double quantum dot Aharonov-Bohm interferometer. The possibility of manipulating the spin current induced by the spin pump effects is explored by tuning the strength γ, the frequency ω, and the direction θ of the rotating magnetic field. Owing to the interdot coupling, two molecular states of the system can be formed. The bonding and antibonding states have a wide and narrow band respectively, resulting an asymmetric structure of the spin current. The number and the location of the spin current peaks depend sensitively on γ and ω. The amplitude of the spin current depends on the field direction θ distinctly. Furthermore, the normal 2π period of the spin current with respect to the magnetic flux can be destroyed by the interdot coupling.

This work is supported by the National Natural Science Foundation of China (Grant Nos. 10704005 and 10574017), and by the Beijing Municipal Science and Technology Commission (Grant No. 2007B017).

References

1. S.A. Wolf, D.D. Awschalon, R.A. Buhrman, J.M. Daughton, S. von Molnar, M.L. Roukes, A.Y. Chtchelkanova, D.M. Treger, Science **294**, 1488 (2001)
2. S.K. Watson, R.M. Potok, C.M. Marcus, V. Umansky, Phys. Rev. Lett. **91**, 258301 (2003)
3. M.J. Stevens, A.L. Smirl, R.D.R. Bhat, A. Najmaie, J.E. Sipe, H.M. van Driel, Phys. Rev. Lett. **90**, 136603 (2003)
4. J. Hübner, W.W. Rühle, M. Klude, D. Hommel, R.D.R. Bhat, J.E. Sipe, H.M. van Driel, Phys. Rev. Lett. **90**, 216601 (2003)
5. S.D. Ganichev, E.L. Ivchenko, S.N. Danilov, J. Eroms, W. Wegscheider, D. Weiss, W. Prettl, Phys. Rev. Lett. **86**, 4358 (2001)
6. E.R. Mucciolo, C. Chamon, C.M. Marcus, Phys. Rev. Lett. **89**, 146802 (2002)
7. W. Zheng, J.L. Wu, B.G. Wang, J. Wang, Q.F. Sun, H. Guo, Phys. Rev. B **68**, 113306 (2003)
8. R. Benjamin, C. Benjamin, Phys. Rev. B **69**, 085318 (2004)
9. A. Brataas, Y. Tserkovnyak, G.E.W. Bauer, B.I. Halperin, Phys. Rev. B **66**, 060404(R) (2002)
10. B. Wang, J. Wang, H. Guo, Phys. Rev. B **67**, 092408 (2003)
11. M. Governale, F. Taddei, Rosario Fazio, Phys. Rev. B **68**, 155324 (2003)
12. A.W. Holleitner, R.H. Blick, A.K. Hüttel, K. Eberl, J.P. Kotthaus, Science **297**, 70 (2002)
13. J.C. Chen, A.M. Chang, M.R. Melloch, Phys. Rev. Lett. **92**, 176801 (2004)
14. D. Loss, D.P. DiVincenzo, Phys. Rev. A **57**, 120 (1998)
15. B. Kubala, J. König, Phys. Rev. B **65**, 245301 (2002)
16. M.L. Ladrón de Guevara, F. Claro, P.A. Orellana, Phys. Rev. B **67**, 195335 (2003)
17. A.P. Jauho, N.S. Wingreen, Y. Meir, Phys. Rev. B **50** 5528 (1994)
18. H. Pan, T.H. Lin, Phys. Rev. B **75**, 195305 (2007)
19. H.K. Zhao, L.N. Zhao, Eur. Phys. J. B **47**, 295 (2005)
20. A. Kogan, S. Amasha, D. Goldhaber-Gordon, G. Granger, M.A. Kastner, H. Shtrikman, Phys. Rev. Lett. **93**, 166602 (2004)
21. P. Zhang, Q.K. Xue, X.C. Xie, Phys. Rev. Lett. **91**, 196602 (2003)
22. Z.T. Jiang, J.Q. You, S.B. Bian, H.Z. Zheng, Phys. Rev. B **66**, 205306 (2002)